Advances and Applications in Mathematical Sciences
Volume 21, Issue 4, February 2022, Pages 2003-2013
© 2022 Mili Publications, India

MATHEMATICAL MODEL OF THE VELOCITY AND TEMPERATURE WITH CONVECTIVE BOUNDARY CONDITIONS: HOMOTOPY ANALYSIS METHOD

M. KARTHIVEL and M. K. SIVASANKARI

Assistant Professor
Department of Mathematics
PSNA College of Engineering and Technology
Dindigul, Tamilnadu, India
E-mail: karthivel.m92@psnacet.edu.in

Assistant Professor
Department of Mathematics
Pasumpon Muthuramalinga Thevar College
Usilampatti, Tamilnadu, India
E-mail: sujipriya18@rediffmail.com

Abstract

This research is aimed at a mathematical model for studying non-linear partial differential equations on velocity and temperature with convective boundary conditions. The Homotopy Analysis method is used to solve the governing nonlinear partial differential equation. To study the behaviours of the different parameters in a graph for velocity and temperature are plotted. The effects of skin friction and the local Nusselt number on various factors are examined and shown in tabular form.

1. Introduction

There are flows that are stimulated not only by differences in temperature but also by differences in concentration in various industrial and real-life problems. The rate of heat transmission is affected by these mass transfer differences. Heat and mass transfer occur in a wide variety of transport processes in industries. Heat and mass transfer is a common

2020 Mathematics Subject Classification: 34Bxx, 76-10, 80A30.
Keywords: Mathematical modeling, Boundary conditions, Casson fluid, Homotopy analysis method, Nusselt number and skin friction.
Received November 9, 2021; Accepted December 6, 2021

occurrence in many chemical processing industries, such as food processing and polymer processing. Many industrial applications, such as fibre and granular insulation, geothermal systems, and so on, are interested in free convection flows [1].

The effects of heat radiation on several fluid flow models were examined by Ibrahim et al. [2] and Aliakbar et al. [3]. Convective heat transfer in M. nanofluid flow is crucial in a variety of engineering applications. Das [4] investigated Cu-water nanofluid's flow and heat transport towards a shrinking sheet in a mixed convection stagnation point. In boundary layer flow, Chaudhary and Merkin [5] looked at homogeneous-heterogeneous reactions. Khan and Pop [6] investigated flow effects on an infinite permeable wall with homogeneous-heterogeneous responses around the two-dimensional stagnation point flow. Mahanta [7] looked into the continuous MHD boundary layer flow of electrically conducting Casson fluid past a shrinking sheet that was exponentially shrinking.

The effects of slip-on unstable mixed convective flow and heat transfer past a stretching surface were discussed by Mukhopadhyay [8]. Lin and Wu [9] investigated simultaneous heat and mass transfer in a vertical plate of laminar free convection boundary-layer flow. The analytical solutions for the boundary layer stagnation point flow and heat transfer towards the shrinking sheet were examined by Bhattacharya et al. [10]. Pavlov [11] investigated the magneto hydrodynamic flow of a viscous incompressible fluid due by surface deformation. The three-dimensional flow caused by a stretching flat surface was studied by Wang [12]. Mehmood and Ali [13] investigated cross-mass transfer phenomena in a lower stretched wall channel. The mass transfer processes in a channel flow across a stretching surface were investigated by Mehmood et al. [14].

The homotopy analysis method (HAM) is employed in this research to establish an analytical expression for the concentration velocity and temperature profile. Furthermore, the Skin Friction analytical solution and the local Nusselt number are explored. The auxiliary parameter in the HAM converges the analytical solution produced. It demonstrates how each of the parameters behaves.

2. Mathematical Formulation

Consider the incompressible flow across a stretching sheet in three dimensions (3D). The sheet is stretched in the xy-plane, while fluid is inserted in the x-axis.

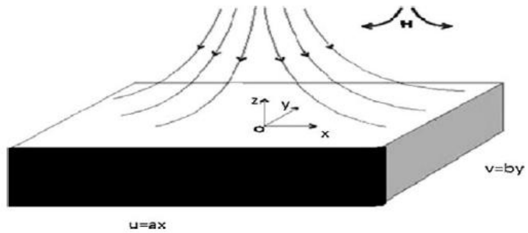

Figure 1. Physical model and coordinate systems [7].

The dimensionless variables for the concentrations in the equations connecting the nonlinear differential equations to the dynamic conditions [7] are introduced as follows:

$$\left(1+\frac{1}{\beta}\right)F''' - (F')^2 - (F + cG)F'' - (M^2 + \lambda)F' = 0 \tag{1}$$

$$\left(1+\frac{1}{\beta}\right)G''' - (G')^2 - (F + cG)\,G'' - (M^2 + \lambda)G' = 0 \tag{2}$$

$$(1 + R)\phi'' - P_r(F + cG)\phi' = 0 \tag{3}$$

where M^2 is the magnetic parameter, P_r is the Prandtl number, $\lambda i\, s$ the porosity parameter, R is the radiation parameter, Biot number (B_i) and stretching parameter (c).

The following boundary conditions are

$$\eta = 0 : F(0) = 0,\ G(0) = 0,\ F'(0) = 1,\ G'(0) = c,\ \phi'(0) = -B_i(1 - \phi(0)) \tag{4}$$

$$\eta = \infty : F'(\infty) = 0,\ G'(\infty) = 0,\ \phi(\infty) = 0 \tag{5}$$

3. Analytical Solutions for the Velocities and Temperature Using Homotopy Analysis Method

The homotopy analysis approach is a semi-analytical tool for solving nonlinear problems. Liao [15] was the first to propose this technique. This method is independent of small/large physical parameters, unlike other analytical techniques. The Homotopy Analysis Method is a simple method for ensuring solution series convergence in a small number of iterations. The approximate analytical expressions obtained by solving the nonlinear equations (2)-(6) using the Homotopy Analysis Method are as follows:

$$F(\eta) = \frac{1}{\sqrt{s}}(1 - e^{-\sqrt{3}\eta}) + \frac{h(c^2+2)}{6s\sqrt{s}}[e^{-2\sqrt{3}\eta} - 2e^{-\sqrt{3}\eta} + 1]$$

$$+ \frac{5k(h-h^2)(M^2c^2 + 2M^2 + \lambda c^2 + 2h) - h^2kc^2(10 - 3c^2) - 2h(1 + c^2)(m^2 + \lambda)}{18s^2\sqrt{s}}$$

$$[1 - 2e^{-\sqrt{s}\eta} + e^{-2\sqrt{s}\eta}] + M\frac{(c^2+2)[4(h-h^2)(m^2+\lambda) - 2h^2(1+c^2)]}{6s^2}$$

$$+ \frac{h^2(c^2+2)(c^2+3)}{26s^2\sqrt{s}}[2 - 3e^{-\sqrt{s}\eta} + e^{-3\sqrt{s}\eta}] \tag{6}$$

$$G(\eta) = \frac{c}{\sqrt{s}}(1 - e^{-\sqrt{s}\eta}) + \frac{h(c^3+2c)}{6s\sqrt{s}}[e^{-2\sqrt{s}\eta} - 2e^{-\sqrt{s}\eta} + 1]$$

$$+ \frac{5k(h-h^2)(M^2c^2 + 2M^2c + \lambda c^2 + 2hc) - h^2kc^2(10 - 3c^2) - 3h(c + c^2)(m^2 + \lambda)}{18s^2\sqrt{s}}$$

$$[1 - 2e^{-\sqrt{s}\eta} + e^{-2\sqrt{s}\eta}] + M\frac{(c^3+2c)[4(h-h^2)(m^2+\lambda) - 2h^2(1+c^2)]}{6s^2}$$

$$+ \frac{h^2c(c^3+2c)(c^2+3)}{26s^2\sqrt{s}}[2 - 3e^{-\sqrt{s}\eta} + e^{-3\sqrt{s}\eta}] \tag{7}$$

$$\phi(\eta) = \frac{B_i(1+R)}{G + B_i(1+R)}e^{-\left(\frac{c}{1+R}\right)\eta} \tag{8}$$

where

$$s = \frac{M^2+\lambda}{k},\ k = 1 + \frac{1}{\beta},\ G = \frac{P_r(1+c^2)}{\sqrt{s}} + \frac{h(c^2+2)(1+c)}{6s\sqrt{s}},\ M\frac{e^{-\sqrt{s}\eta} - 1}{\sqrt{s}} + xe^{-}$$

The dimensionless local Nusselt number and skin friction are as follows for analytical expressions [7]:

$$\mathrm{Re}_x^{1/2}\, C_{fx} = \left(1 + \frac{1}{\beta}\right) F''(0) \tag{9}$$

$$\mathrm{Re}_x^{1/2}\, C_{fy} = \left(1 + \frac{1}{\beta}\right) F''(0) \tag{10}$$

where $C_{fx} = \dfrac{\tau_{wx}}{\rho u_w^2}$, $C_{fy} = \dfrac{\tau_{wx}}{\rho u_w^2}$

C_f is the skin friction, C_{fx} and C_{fy} are skin friction along the x-and y-directions τ_{wx} and τ_{wy} are defined.

$$\mathrm{Re}_x^{-1/2}\, Nu = -\phi(0) \tag{11}$$

where $\mathrm{Re}_x = u_x(x)\, x/\upsilon$ is defined.

4. Result and Discussion

The analytical expression of velocities and temperature is represented by equations (1)-(5). The velocity and temperature profile for various values of physical parameters $M, \lambda, \beta, B_i, P_r, R$ and C have been studied in this paper. The obtained analytical results in Figures 2 to 10 for various values of parameters. It agrees well with the earlier result as well as the numerical result [7].

The fluid velocity is depicted in Figures 2 to 4 for various parameter values.

As the casson parameter improves, the influence of the velocity $F'(\eta)$ decreases, as seen in Figure 2. In Figure 3, it can be seen that as the parameter is increased, the velocity decreases. The impacts of parameters M and C on the velocity profiles have been displayed in Figure 4. The fluid velocity decreases as M and C increase, as seen in the graph.

Examine the velocity profile in Figures 5 and 6 for various values of parameters λ and β. It is observed that as the parameters and is reduced, the improves the velocity profile $G'(\eta)$. The influence of M and C on the velocity profiles is shown in Figure 7. It is noticed that as the fluid's velocity $G'(\eta)$ decreases, M increases. It's evident that when the velocity profile increases and also parameter C increases.

It is shown in Figure 8 to study the effects of $\phi(\eta)$ on temperature. It is obvious that when temperature rises, the parameter P_r. decreases. The temperature profile $\phi(\eta)$ is influence of the various values of parameters B_i is shown in Figure 9. This is due to the fact that when the parameter B_i increases, so does the $\phi(\eta)$ temperature. It is obvious from Figure 10 that as the parameter R increases, the temperature profile $\phi(\eta)$ similarly increases.

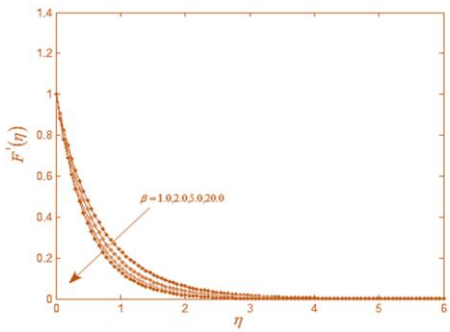

Figure 2. Analytical expression of dimensionless concentration in velocity $F'(\eta)$ versus η at various values of β for fixed values of parameters $M = 2$, $C = 0.5$, $\lambda = 0.5$, $h = -0.1$.

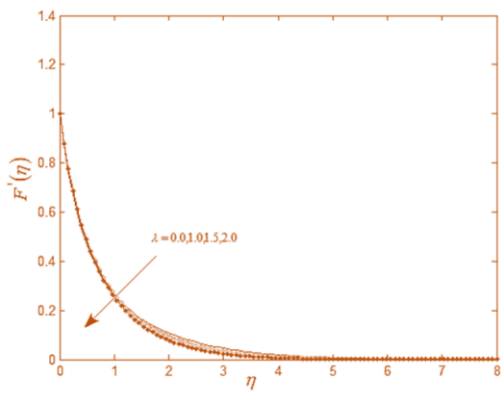

Figure 3. Analytical expression of dimensionless concentration in velocity $F'(\eta)$ versus η at various values of λ for fixed values of parameters $M = 2$, $C = 0.5$, $\beta = 0.5$, $h = -0.1$.

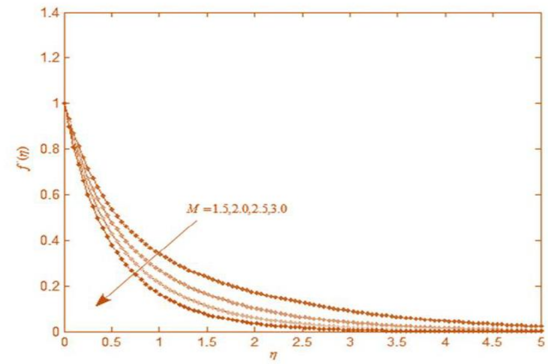

Figure 4. Analytical expression of dimensionless concentration in velocity $F'(\eta)$ versus η at various values of M for fixed values of parameters $\lambda = 0.5$, $C = 0.5$, $\beta = 0.5$, $h = 0.1$.

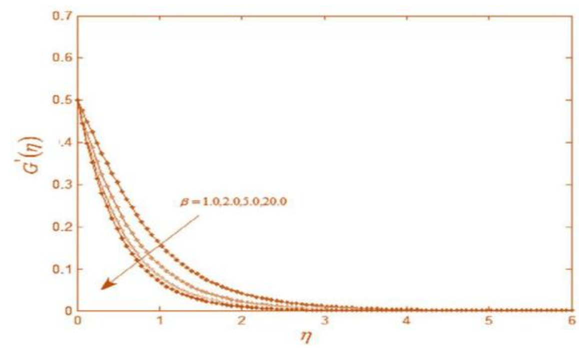

Figure 5. Analytical expression of dimensionless concentration in velocity $G'(\eta)$ versus η at various values of λ for fixed values of parameters $M = 2$, $C = 0.5$, $\lambda = 0.5$, $h = 0.1$.

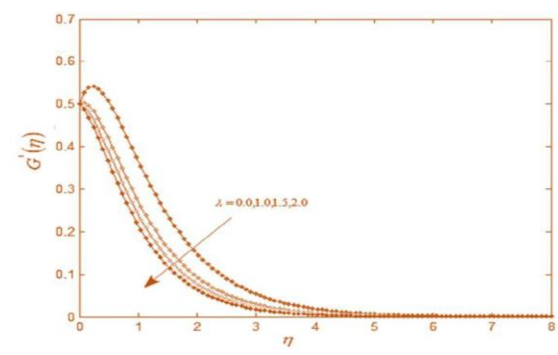

Figure 6. Analytical expression of dimensionless concentration in velocity $G'(\eta)$ versus η at various values of λ for fixed values of parameters $M = 2$, $C = 0.5$, $\beta = 0.5$, $h = 0.1$.

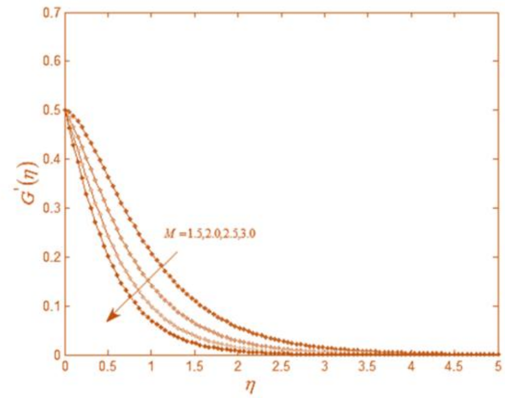

Figure 7. Analytical expression of dimensionless concentration in velocity $G'(\eta)$ versus at η various values of M for fixed values of parameters $\lambda = 0.5$, $C = 0.5$, $\beta = 0.5$, $h = 0.1$.

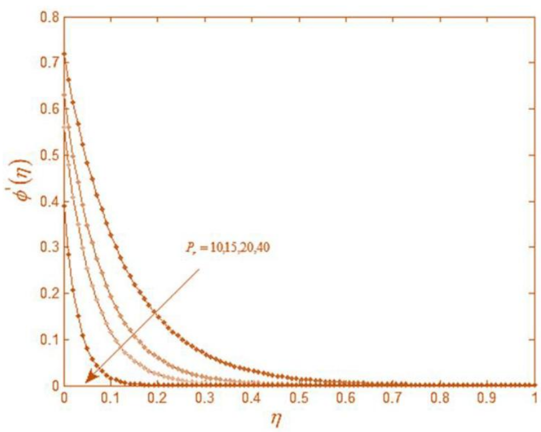

Figure 8. Analytical expression of dimensionless concentration in temperature $\phi(\eta)$ versus η at various values of P_r for fixed values of parameters $M = 2$, $\lambda = 0.5$, $C = 0.5$, $R = 0.3$, $B_i = 20$, $\beta = 0.5$, $h = 0.1$.

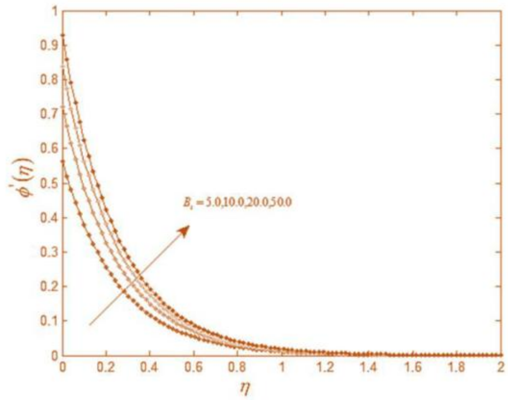

Figure 9. Analytical expression of dimensionless concentration in temperature $\phi(\eta)$ versus η at various values of P_r for fixed values of parameters $M = 2$, $\lambda = 0.5$, $C = 0.5$, $R = 0.3$, $\beta = 0.5$, $P_r = 5$, $h = 0.1$.

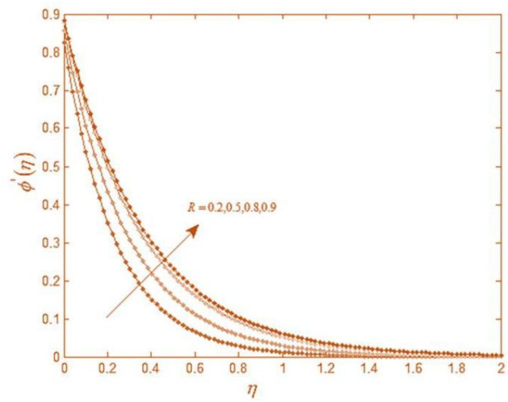

Figure 10. Analytical expression of dimensionless concentration in temperature $\phi(\eta)$ versus η at various values of R for fixed values of parameters $M = 2$, $\lambda = 0.5$, $C = 0.5$, $B_i = 20$, $\beta = 0.5$, $P_r = 5$, $h = 0.1$.

5. Conclusion

This paper describes a mathematical model of concentration in a velocity and temperature profile that has been used to investigate many features of the Casson fluid. We also examined the effect of a wide range of physical parameters on model prediction. The nonlinear partial differential equations system is solved using the Homotopy Analysis Method. Furthermore, for velocities, and temperature, effects for various values of emerging parameters are examined. Both the temperature distribution and the volume fraction are reversed when the Prandtl number and the Lewis number are used.

References

[1] B. Awasthi, Effects of heat and mass flux on MHD free convection flow through a porous medium with radiation and first order chemical reaction, Int. J. of Applied Mechanics and Engineering 23(4) (2018), 855-871.

[2] F. S. Ibrahim, A. M. Elaiw and A. A. Bakr, Effect of chemical reaction and radiation absorption on the un-steady MHD free convection flow past a semi-infinite vertical permeable moving plate with heat source and suction, Comm. Nonlin. Sci. Num. Simul. 13(6) (2008), 1056-1066.

[3] V. Aliakbar, A. Alizadeh-Pahlavan and K. Sadeghy, The influence of thermal radiation on MHD flow of maxwellian fluids above stretching sheets, Communications in Nonlinear Science and Numerical Simulation 14(3) (2009), 779-794.

[4] K. Das, Mixed convection stagnation point flow and heat transfer of cu-water nanofluids towards a shrinking sheet, Heat Trans. Asian Res. 42(3) (2013), 230-242.

[5] M. A. Chaudhary and J. H. Merkin, A simple isothermal model for homogeneous-heterogeneous reactions in boundary layer flow: I. equal diffusivities, Fluid Dynam. Res. 16 (1995), 311-333.

[6] W. A. Khan and I. Pop, Flow near the two-dimensional stagnation point on a infinite permeable wall with a homogeneous-heterogeneous reaction, Comm. Nonliear. Sci. Numer. Simulat. 15 (2010), 3435-3443.

[7] G. Mahanta and S. Shaw, 3D Casson fluid flow past a porous linearly stretching sheet with convective boundary condition, Alexandria Engineering Journal 54 (2015), 653-659.

[8] S. Mukhopadhyay, Effects of slip on unsteady mixed convective flow and heat transfer past a stretching surface, Chin. Phys. B. 27 (2010), 256-307.

[9] H. T. Lin and C. M. Wu, Combined heat and mass transfer by laminar natural convection from a vertical plate, Heat and Mass Transfer 30 (1995), 369-376.

[10] K. Bhattacharyya, S. Mukhopadhyay and G. C. Layek, Slip effects boundary layer stagnation-point flow and heat transfer towards a shrinking sheet, J. Heat Mass Transf. 54 (2011), 308-313.

[11] K. B. Pavlov, Magneto hydrodynamic flow of an incompressible viscous fluid caused by deformation of a surface, Magn. Gidrodin. 4 (1974), 146-147.

[12] C. Y. Wang, The three dimensional flow due to a stretching flat surface, Phys. Fluids 27 (1984), 1915-1917.

[13] A. Mehmood and A. Ali, Across mass transfer phenomena in a channel of lower stretching wall, Chem. Eng. Commun. 198 (2011), 678-691.

[14] A. Mehmood, S. Munawar and A. Ali, Cooling of hot stretching surface in the presence of

across mass transfer phenomena in a channel flow, Z. Naturforschung 69 (2014), 21-33.

[15] S. J. Liao, The Proposed Homotopy Analysis Technique for the Solution of Nonlinear Problems, Ph. D. Thesis, Shanghai Jiao Tong University, (1992).

[16] M. K. Sivasankari and M. Karthivel, Analytical solution of steady state substrate concentration of an immobilized enzyme kinetics by Adomian decomposition method, Advances and Applications in Mathematical Sciences 18(10) (2019), 1063-1070.

[17] M. K. Sivasankari and I. Athal, Mathematical models of solving partial differential equations in variational iteration method, Advances and Applications in Mathematical Sciences 18(10) (2019), 1087-1092.

[18] I. Athal and M. K. Sivasankari, Theoretical analysis for chemical kinetics system using Laplace transform method, European Journal of Molecular and Clinical Medicine 7(11) (2020), 1708-1713.

[19] M. Karthivel and M. K. Sivasankari, Mathematical modeling for 2-D fluorescence spectra based using Laplace transform method, European Journal of Molecular and Clinical Medicine 7(11) (2020), 1739-1743.

[20] I. Athal and M. K. Sivasankari, Approximate solutions of transient free-convective flow in a vertical channel due to symmetric heating using Laplace transform technique, International Journal of Modern Agriculture 10(1) (2021), 163-167.